IOP Publishing
Journal of Micromechanics and Microengineering
J. Micromech. Microeng. 27 (2017) 045003 (10pp)
doi:10.1088/1361-6439/aa5d70

Low-power catalytic gas sensing using highly stable silicon carbide microheaters

Anna Harley-Trochimczyk[1,2], Ameya Rao[1,2], Hu Long[1,2], Alex Zettl[3,4,5], Carlo Carraro[1,2] and Roya Maboudian[1,2]

[1] Department of Chemical and Biomolecular Engineering, University of California at Berkeley, Berkeley, CA 94720, United States of America
[2] Berkeley Sensor & Actuator Center, University of California at Berkeley, Berkeley, CA 94720, United States of America
[3] Department of Physics, University of California at Berkeley, Berkeley, CA 94720, United States of America
[4] Materials Science Division, Lawrence Berkeley National Laboratory, Berkeley, CA 94720, United States of America
[5] Kavli Energy NanoSciences Institute at the University of California, Berkeley and the Lawrence Berkeley National Laboratory, Berkeley, CA 94720, United States of America

E-mail: maboudia@berkeley.edu

Received 16 August 2016, revised 14 January 2017
Accepted for publication 1 February 2017
Published 21 February 2017

Abstract
A robust silicon carbide (SiC) microheater is used for stable low-power catalytic gas sensing at high operating temperatures, where previously developed low-power polycrystalline silicon (polysilicon) microheaters are unstable. The silicon carbide microheater has low power consumption (20 mW to reach 500 °C) and exhibits an order of magnitude lower resistance drift than the polysilicon microheater after continuously heating at 500 °C for 100 h and during temperature increases up to 650 °C. With the deposition of platinum nanoparticle-loaded boron nitride aerogel, the SiC microheater-based catalytic gas sensor detects propane with excellent long-term stability while exhibiting fast response and recovery time (~1 s). The sensitivity is not affected by humidity, nor during 10% duty cycling, which yields a power consumption of only 2 mW with frequent data collection (every 2 s). With a simple change of heater material from silicon to SiC, the microheater and resulting catalytic gas sensor element show significant performance improvement.

Keywords: gas sensor, silicon carbide, microheater, catalytic gas sensor, boron nitride aerogel, combustible gas

(Some figures may appear in colour only in the online journal)

1. Introduction

Combustible gases such as hydrogen and hydrocarbons are prevalent in industrial environments. More ubiquitous atmospheric monitoring of these gases would allow for faster leak detection, which would result in increased worker safety and reduced damage to equipment and the environment. However, installation of a fixed gas monitor in a class 1 or 2 hazardous facility can be expensive. Wireless, battery-powered gas monitors would eliminate the bulk of the installation costs, but have power constraints that current combustible gas sensing technology cannot meet. Development of a low-power catalytic sensor with competitive performance characteristics is the critical step in allowing for ubiquitous combustible gas monitoring.

The main reason for the high power consumption of the current sensor components is the need for the catalyst to be heated to high temperatures (~500 °C). To minimize the power consumption, two main strategies have been proposed: (1) miniaturization through the use of microfabricated heaters, and (2) reduction of the combustion temperature. Research efforts on efficient low-temperature hydrocarbon combustion

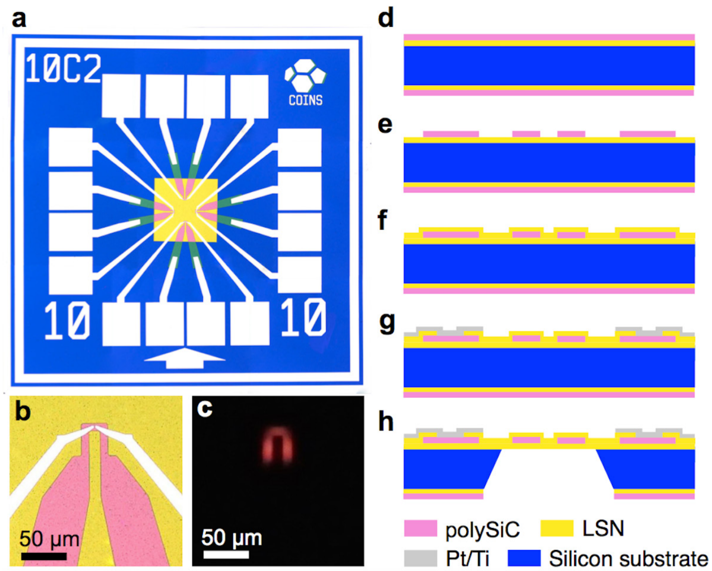

Figure 1. (a) Optical image of four SiC microheaters on the chip ($3.5 \times 3.5\,\mathrm{mm}^2$). (b) Close-up of one microheater. (c) Microheater powered to glowing, showing hot zone. (d)–(h) Overview of microheater fabrication process. (d) Low pressure chemical vapor deposition of a low-stress silicon nitride (LSN) layer and doped polycrystalline silicon carbide layer. (e) polySiC is patterned with photolithography and plasma etched to form the microheaters. (f) Deposition of a second LSN layer encapsulates the microheaters. (g) After etching a window in the top LSN layer, Pt/Ti metal contacts are created through photolithography, evaporation, and lift-off. (h) A window is etched in the back-side of the wafer to expose the silicon substrate, which is anisotropically etched with hot KOH to release the membrane.

have not yielded promising results [1, 2]; thus research focus has been on the use of microheaters as the catalytic gas sensor platform [3–6]. A microfabricated sensor platform can leverage silicon micromachining processes for low cost and reproducible manufacturing. Microheaters have been fabricated from a variety of materials, most commonly polysilicon or platinum, and consist of a heater trace thermally isolated from the substrate via a thin membrane of silicon nitride or silicon dioxide. Joule heating is used to reach the desired operating temperatures.

Although progress has been made in minimizing the power consumption of these microheaters, deployment of microheater-based catalytic gas sensors is contingent on obtaining stable, reproducible measurements in field conditions. Platinum and polysilicon microheaters both suffer from instability when operated at the high temperatures required for catalytic gas sensing. Platinum suffers from electromigration, poor adhesion to the most common membrane materials [7, 8], and oxidation if it is not isolated from the atmosphere. The resistance of polysilicon is not very stable as it approaches the recrystallization temperature (~600 °C [9]), where grains can coalesce and cause long-term drift [10–12]. Especially considering that 500 °C is the baseline operating temperature and the temperature increases in the presence of combustible gas, these materials suffer from severe drawbacks for long-term use.

Silicon carbide has been investigated as an advantageous material for microelectronics and microsensors involving high temperature operation [13, 14]. The robust performance of silicon carbide at high temperature makes it an attractive replacement for polysilicon [13]. Silicon carbide has been used in microheater fabrication, both as a membrane material since its high thermal conductivity leads to better temperature uniformity across the device [15–19], and as the microheater material itself [14, 16, 20–23]. SiC microheaters have demonstrated robust behavior in high temperature applications [14, 23], including for metal oxide-based gas sensing [16, 17], but their use for catalytic gas sensing is not reported to-date.

In this paper, we report the development of a low-power silicon carbide microheater, requiring only 20 mW to reach 500 °C [24, 25]. Comparison of the SiC microheater to a polysilicon microheater with the same dimensions shows significant improvements in baseline resistance stability for operation at 500 °C and above. With the integration of an advanced catalytic material, platinum nanoparticle-loaded boron nitride aerogel, the SiC microheater platform can be used for propane detection with high sensitivity, fast response and recovery (~1 s) and highly stable response. Additionally, the sensitivity is unaffected by humidity and 10% duty cycling, so the power consumption can be decreased to only 2 mW with data still collected every 2 s. These developments offered by the silicon carbide microheater can unlock the true potential of low power catalytic gas sensing for wireless applications.

2. Materials and methods

2.1. Microheater fabrication

The microheater platform consists of a back-etched silicon nitride membrane encapsulating four microheater elements on a single chip that is $3.5 \times 3.5\,\mathrm{mm}^2$ in size (figure 1(a)). The thin membrane provides the microheaters with thermal isolation from the substrate to keep the power consumption low requiring only 20 mW to reach 500 °C. Because the silicon

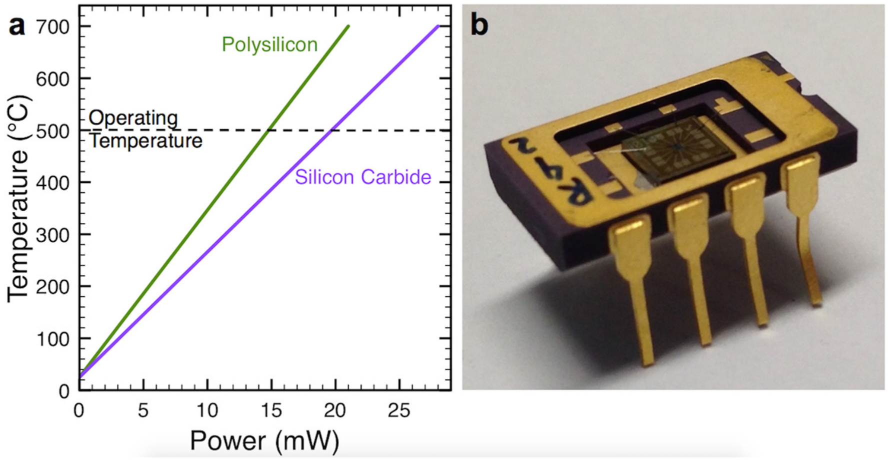

Figure 2. (a) Power temperature relationship for the polysilicon and SiC microheaters. (b) Optical image of packaged microheater chip ready for sensor testing.

nitride layers are optically transparent, the encapsulated SiC trace (pink) can be seen in figure 1(b). The two Pt/Ti sensing electrodes (white) are not used in this work and are masked with a thin layer of silicon dioxide before sensor testing to avoid interference from the platinum. Figure 1(c) shows an optical image of the microheater powered to the point where it is glowing, which shows that the hot zone is the thinnest part of the trace, giving an approximately 50×50 μm^2 heated area. Figure 1(h) shows a cross-sectional schematic of the microheater with the closed membrane configuration and metal contacts placed off the membrane to keep them cool and hence, avoid stability issues associated with metal contacts at elevated temperatures. The closed membrane assists with integration of the sensing material by providing a flat surface for deposition.

The silicon carbide fabrication process follows the previously developed polysilicon microheater fabrication, described in detail elsewhere [24, 26]. To facilitate comparison, only the deposition and etch chemistries for the silicon carbide steps are changed. Briefly, the deposition of a 100 nm low-stress silicon nitride (LSN) layer on a 4 inch p-type double-side polished silicon wafer is followed by the silicon carbide film deposition (figure 1(d)). The SiC film is deposited using methylsilane, hydrogen, and dichlorosilane as precursors in a low-pressure (170 mTorr) hot-wall reactor at $T = 835$ °C with a dopant source of ammonia gas and with the wafers in a closed-boat geometry with slots to limit the gas diffusion and improve the film uniformity [27]. The deposited film is polycrystalline cubic 3C-SiC with a sheet resistivity of 5700 Ω/square and a thickness of 130 nm. To define the microheaters (figure 1(e)), the wafer is patterned with photolithography employing positive photoresist (FujiFilm OiR 906-12) with a thickness of ~1.2 μm as the mask. To selectively remove the SiC, reactive ion etching is done with HBr and Cl_2 gases using a transformer coupled plasma system [28]. A high power of 300 W is needed to have an appreciable etch rate (~1.5 nm s^{-1}), hence the etching is done in 10 s increments to prevent overheating of the photoresist mask. A second silicon nitride layer with the thickness of 100 nm is deposited to encapsulate the microheaters (figure 1(f)). After etching a window in the top LSN layer, the metal contacts are defined through photolithography, evaporation of 90 nm Pt on a 10 nm Ti adhesion layer and lift-off in acetone (figure 1(g)). Finally, a window is plasma-etched on the back-side of the wafer to expose the silicon substrate, which is etched in a KOH bath (24 wt%) at 80 °C with bubbled oxygen to release the membrane (figure 1(h)). The front-side of the wafer is protected with an alkaline resistant coating (Brewer Science, Protek B3) during the KOH etch. The protective coating is kept in place during the dicing process and removed from individual chips before use.

2.2. Microheater testing

The microheater testing is done with a Keithley 2602A source-meter. The current–voltage measurements are taken using LabTracer 2.9 software. The continuous and variable temperature tests are taken with an open-source Java-based program called Zephyr. Modeling conduction with Fourier's law gives a linear relationship between applied power and the temperature difference between the microheater and room temperature (figure 2(a)). Convection through the air is minimal with the small element size. Radiation modeled based on the Stefan Boltzmann law of blackbody radiation follows $P = A\sigma\varepsilon\Delta T^4$, which is highly non-linear. However, assuming an emissivity, ε, of 1 and a hot area, A, of 50×50 μm, the radiative power barely reaches ~0.1 mW at 700 °C, which is less than 1% of the total applied power. Even considering the radiative loss in the surrounding membrane, assuming a temperature profile that scales logarithmically from the hot area, results in an estimate of radiative power less than 5% of the total applied power. Therefore, in the operating temperature range of the microheater, radiative effects can be considered to be negligible. Given the linear relationship between applied power and temperature, the temperature can be defined with two calibration points. The first is at room temperature and the second is done by powering the heater to the glowing point and then fitting the emission spectrum with a Planck distribution [26, 29]. The emitted spectrum over a range of wavelengths is collected using a spectrometer

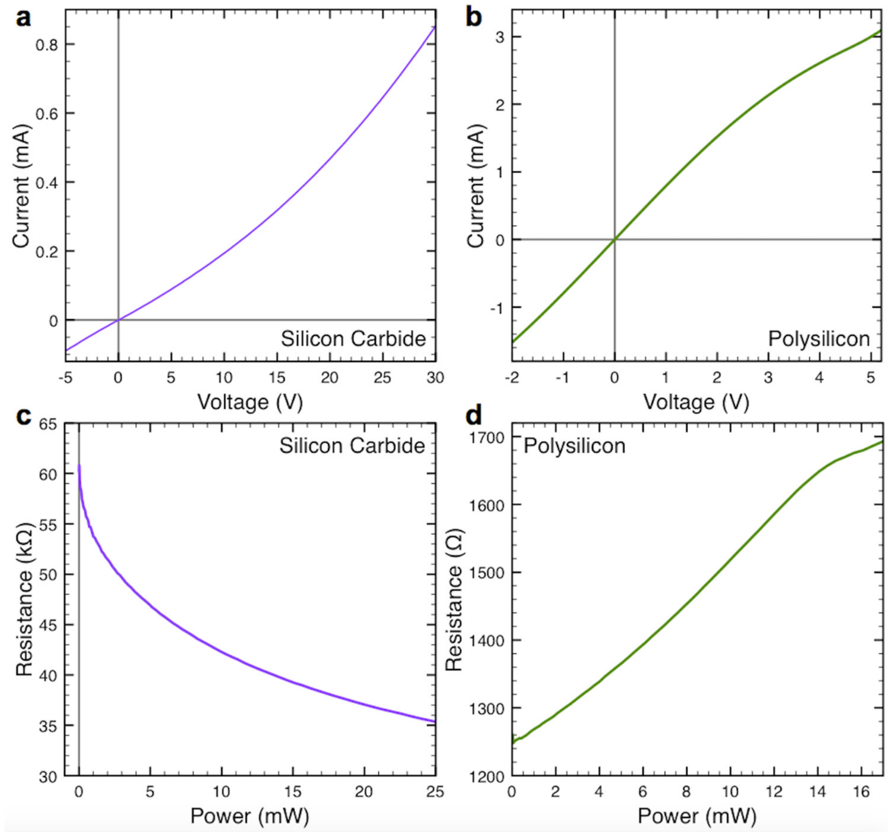

Figure 3. Current–voltage sweeps for (a) SiC and (b) polysilicon microheaters. Resistance versus power relationship calculated from the current–voltage sweep for (c) SiC and (d) polysilicon microheaters. To reach 500 °C, the applied power for (c) SiC microheater is 20 mW and (d) polysilicon microheater is 15 mW.

with a small spot area focused on the hottest area. The onset of visible glow is found to be ~700 °C which is 21 mW for the polysilicon microheaters and 28 mW for the SiC heaters. Although measuring the heater resistance during external heating is a common temperature calibration technique, it is not accurate for this microheater platform because the colder parts of the heater contribute a non-negligible portion of the total resistance. Therefore, external heating where the entire chip is at a given temperature does not provide the same resistance as when only the hot zone of the microheater is at that temperature.

2.3. Sensor fabrication and testing

The platinum nanoparticle-loaded boron nitride aerogel (Pt-BN) synthesis and characterization can be found in full detail in [25]. Scanning electron microscopy imaging is done with a Zeiss LEO 1550 system to observe the aerogel morphology. For sensor testing, a microheater chip is wire-bonded into a ceramic dual in-line package (figure 2(b)). The Pt-BN is suspended in isopropyl alcohol (IPA) with sonication and a few microliters are dropped onto the chip while the microheater is heated to the boiling point of IPA (80 °C) to facilitate local deposition. The packaged sensor is exposed to the gases of interest in a 1 cm^3 Teflon chamber. Propane (5% in N_2, Praxair), oxygen, and nitrogen gas flow rates are set by a Labview program that controls Bronkhurst mass flow controllers. The oxygen concentration is kept constant at 20% with nitrogen as the balance and the total gas flow rate is set to 300 sccm. A Keithley 2602A source-meter and Zephyr software are used to apply a given potential to the sensor and record the sensor resistance in response. Sensing response is reported as $(R_{gas} - R_0)/R_0 \times 100\%$ where R_{gas} is the sensor resistance during exposure to a given concentration of gas and R_0 is the sensor resistance in synthetic air only.

3. Results and discussion

3.1. Microheater characterization

The current–voltage sweeps of the SiC and polysilicon microheaters are shown in figures 3(a) and (b). The resistance versus power relationship is calculated from the current–voltage sweep and plotted in figures 3(c) and (d). Because the power is linearly proportional to the heater temperature in the range up to 700 °C, the resistance-power relationship is functionally the same as the resistance-temperature relationship. The SiC microheaters have a higher resistance at room temperature, about 60 kΩ compared to 1.25 kΩ for the polysilicon microheaters. The SiC microheaters require a higher applied voltage

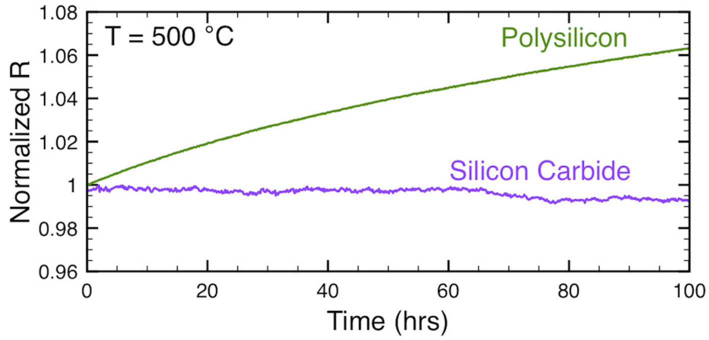

Figure 4. Normalized resistance of polySiC and polysilicon microheaters continuously powered to 500 °C for 100 h.

to reach the same power as the polysilicon microheater, which is the reason for the potential sweep extending to 30 V compared to 5 V for polysilicon. The required voltage for the silicon carbide microheater is higher than a typical voltage supply for wireless sensors can deliver, but this may be improved with further optimization of the silicon carbide doping, as well as decreasing the total membrane thickness. To reach 500 °C, the polysilicon microheater requires 15 mW while the SiC microheater requires 20 mW, which is attributable to the higher thermal conductivity of SiC compared to polysilicon [13]. With a higher thermal conductivity, the silicon carbide trace can sink more heat into the substrate, lowering the heating efficiency and increasing the power required to reach a given temperature.

As is evident from figures 3(c) and (d), the two microheaters have temperature coefficients of resistance that are opposite in sign and non-linear, with the polysilicon resistance increasing with temperature and the SiC resistance decreasing with temperature. With the heater at 500 °C, the calculated TCR values are +350 ppm K^{-1} for polysilicon and −700 ppm K^{-1} for polySiC. The magnitude and sign of the SiC TCR are comparable to prior reports [21, 30]. The sign of the microheater TCR is controlled by the competing effects of increased phonon scattering in the crystal grain leading to an increasing resistance with temperature, and thermal activation of carriers across the grain interfaces leading to a decreasing resistance with temperature. The change in slope observed in polysilicon at 14 mW coincides with the recrystallization temperature. Because the magnitude of the SiC TCR is twice as large as the polysilicon, the same change in temperature due to gas combustion results in a larger resistance change from SiC than from polysilicon, making it a more sensitive transducer for catalytic gas sensing.

When both microheaters are continuously powered at 500 °C for 100 h (figure 4), the SiC microheater shows an order of magnitude lower drift (−0.6%) than the polysilicon (7%). The resistance of each microheater is normalized to the initial value for easier comparison. The SiC microheater displays a higher noise level, possibly due to the lower current level used to reach the operating temperature. Previous reports have also shown long-term positive resistance drift in polysilicon microstructures at temperatures close to 500 °C [9, 11], and suggest the cause may be dopant segregation at grain boundaries or dopant diffusion along the temperature gradient. Some decrease in the rate of drift is observed over the first 100 h, suggesting that with a long 'burn-in' or conditioning time, the drift could be mitigated. However, during catalytic gas sensing, the combustion of the target gas leads to an increase in temperature above the 500 °C heater baseline; thus the microheater behavior must be stable with changing high temperature as well as with a constant baseline.

To demonstrate this issue, applying a set of temperatures from 510 to 650 °C with a baseline of 500 °C (figure 5(a)) results in major instability in the polysilicon microheater, including history dependence (figure 5(b)) where the response depends on what temperatures are previously reached. The recrystallization temperature of polysilicon is around 600 °C [9]; thus the resistance decrease when the microheater is held at the highest temperature may be due to grain growth. During the return to baseline, the resistance increases again just as with the long-term drift observed in figure 4. In a previous report, the resistance of a polysilicon heater at low temperature depends on the high temperature previously reached and the cooling rate [9]. In the temperature profile applied in figure 5(a), the temperature switching is done in the same length of time but with different temperature changes, so the cooling rate differs for each temperature reached. This may explain why the polysilicon microheater returns to different resistance values after reaching various elevated temperatures. In contrast to this unpredictable behavior, the SiC microheater displays stable baseline recovery even when heated to 650 °C (figure 5(c)) as well as stable resistance values when the temperature is held constant at a particular value. The high chemical stability and wide bandgap of silicon carbide microheater make it highly resistant to thermally induced resistance drift, which makes it the superior choice for a sensing platform with high operating temperature.

3.2. Catalytic gas sensing response

With the addition of Pt-BN as the catalytic material (figure 6(a)), the SiC platform can be used for catalytic gas sensing. Figure 6(a) shows the Pt-BN after drop-casting on top of the silicon carbide microheater. As a commonly used fuel, refrigerant, and process chemical, propane is used to demonstrate the sensor performance [31, 32]. Although the auto-ignition temperature for propane is 450 °C, there is no response from the bare microheater. Other researchers have shown that small

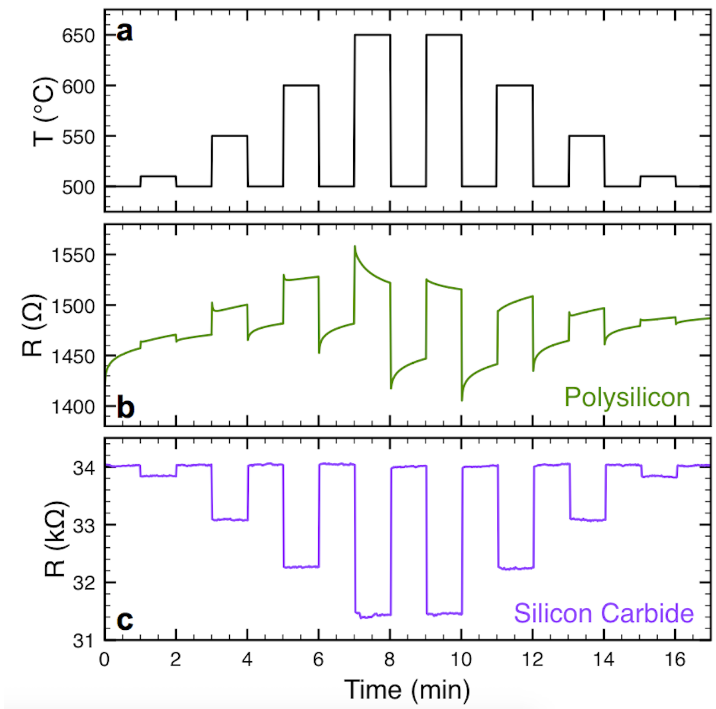

Figure 5. (a) Temperature profile applied to the microheaters and resulting (b) polysilicon and (c) polySiC microheater resistance.

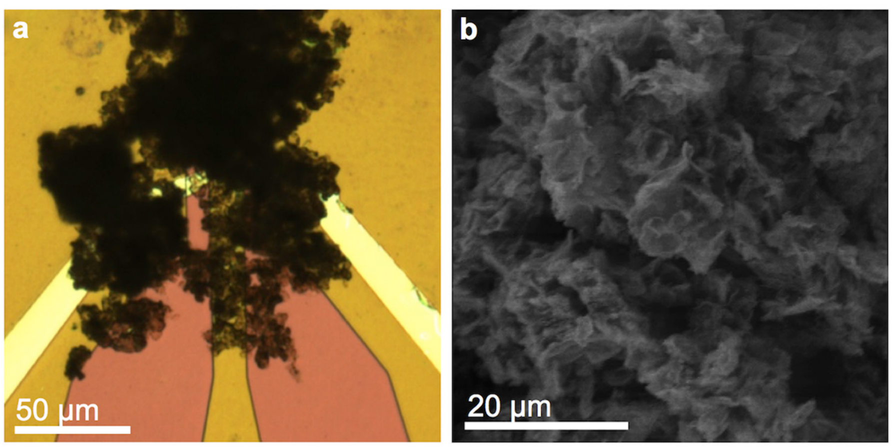

Figure 6. (a) Optical image of the Pt-BN catalyst after drop-casting on top of the microheater. (b) SEM image of the Pt-BN showing the high surface area morphology.

microheater-based sensors are inherently explosion-proof without expensive packaging [33]. The lower explosive limit (LEL), defined as the lowest concentration capable of producing an explosion, for propane is 2.1% or 21 000 ppm; thus, the sensor is exposed to concentrations below that value. As shown in previous work [25], the sensors made with bare boron nitride aerogel do not show any propane response, indicating the platinum nanoparticles are required for gas combustion.

The SEM image of the Pt-BN in figure 6(b) shows the high surface area morphology of the material. The transmission electron microscopy analysis reported previously indicates that the average Pt nanoparticle diameter is 17 nm and the platinum is crystalline and well-adhered to the boron nitride aerogel [25]. Earlier analysis also shows that the boron nitride aerogel scaffold is 7–10 layers thick and the specific surface area is calculated to be 450 $m^2\ g^{-1}$ before platinum loading using nitrogen adsorption [25]. The high specific surface area allows for high nanoparticle loading with minimal support mass, improving the transfer efficiency of the heat generated during hydrocarbon combustion and the response time. The boron nitride aerogel scaffold is chosen because of the improved thermal stability it gives over graphene aerogel.

Figure 7(a) shows the effect of temperature on sensor response to 2% propane, where the response is defined as the percentage change in resistance. The figure shows that above 300 °C, the propane response monotonically increases with

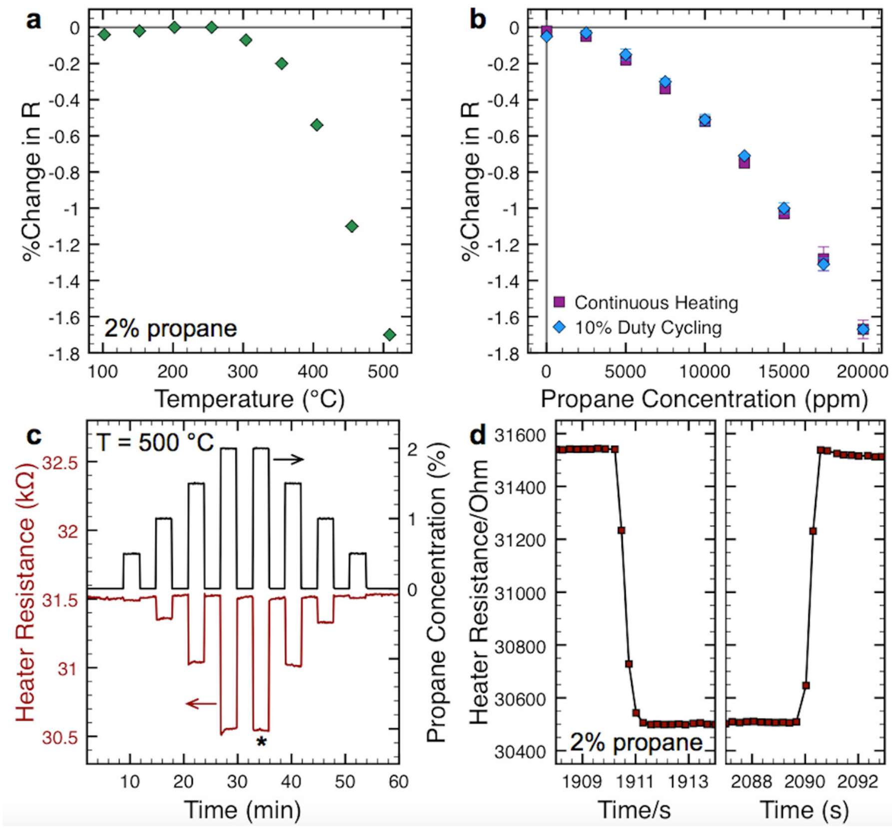

Figure 7. (a) Pt-BN SiC sensor response to 2% or 20 000 ppm propane at various operating temperatures. (b) Sensitivity of the Pt-BN SiC sensor during continuous heating at 500 °C compared to 10% duty cycling with the heater on for 0.2 s every 2 s. (c) Response to varied propane concentrations versus time at 500 °C showing good baseline stability and response reproducibility. (d) Pt-BN SiC sensor response and recovery time for 2% propane ($t_{90} < 1$ s) at 500 °C.

temperature. Even at 500 °C, the sensor has not reached a mass-transfer limited regime, beyond which point the sensitivity is expected to not change as strongly with temperature. Operating in a kinetically-limited regime impacts the linearity of the response with concentration, because as the sensor responds and heats up, the rate of reaction increases, leading to further increase in the temperature and rate. This explains the nonlinearity seen in the response versus concentration curve in figure 7(b). Operating at higher temperatures in order to reach a mass-transfer limited regime is possible with the silicon carbide microheater, but the power consumption increases. Also, as temperature increases above 700 °C, the relationship between power and temperature starts to become non-linear as radiative heat loss becomes more significant, making it much more difficult to interpret the signal.

The Pt-BN SiC sensor resistance shown in figure 7(c) with varied propane gas exposure shows a high degree of stability in the baseline and reproducibility in response. In between the propane exposures, clean, dry synthetic air is flown over the sensor. Exposure to 20 000 ppm propane results in an approximately 65 °C increase of the microheater temperature, as estimated from the resistance versus temperature calibration curve, but the sensor recovers well to the baseline after gas exposure. Using a signal-to-noise ratio of 3, the limit of

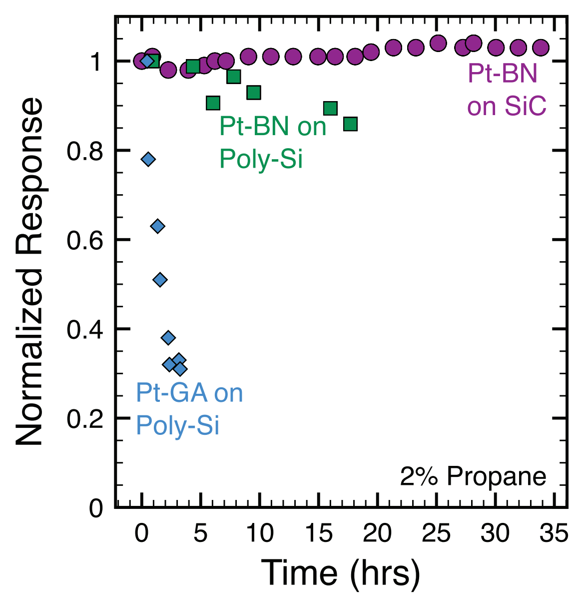

Figure 8. Pt-BN SiC sensor response to 2% propane over 36 h of operation compared to Pt-BN, Pt-GA, and a Pt thin film on the polysilicon microheater.

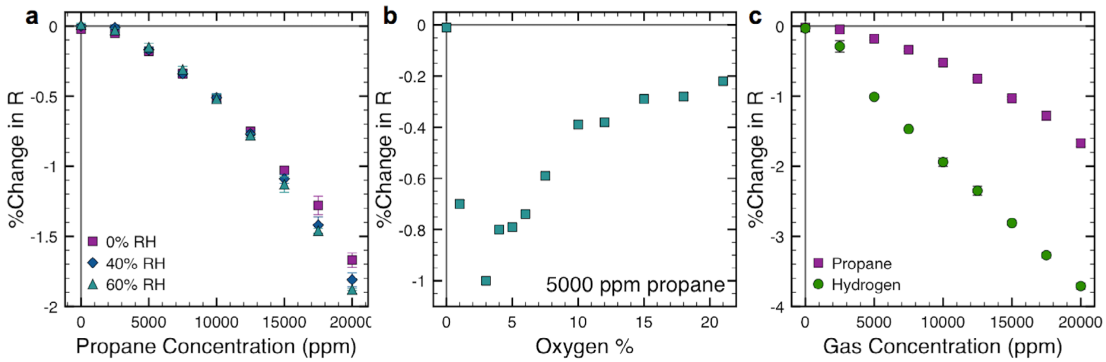

Figure 9. (a) Pt-BN SiC sensor response to propane at 500 °C with varying levels of relative humidity. (b) Sensor response to 5000 ppm propane with varied oxygen concentration. (c) Comparison of Pt-BN SiC sensor response to propane and hydrogen.

detection is calculated to be 3420 ppm propane at the operating temperature of 500 °C. Given that the lower explosive limit for propane is 21 000 ppm, the sensing range of the device is quite respectable and comparable to other literature reports for microcatalytic propane detection [4, 33]. The sensor response is very fast, comparable to the previous results using the polysilicon microheater [24, 26]. Figure 7(d) shows a zoomed-in view of the starred response in figure 7(c) for the start of exposure to 2% propane and the recovery when the gas is switched back to clean air. The times to reach 90% of the full signal level (t_{90}) for response and recovery of the sensor are ~1 s, which is similar to results reported for the Pt-BN polysilicon sensor [25]. In the quest for a battery-powered combustible gas sensor, decreasing the power consumption through duty cycling, or only powering the heater for short bursts, is a useful strategy. However, larger heater elements with a slower response time only allow infrequent data collection or do not reach the full operating temperature during duty cycling and the sensitivity suffers. Here, the heater is turned on for 200 ms every 2 s with no change in the sensitivity compared to continuous heating at 500 °C (figure 7(b)) and the data collection remains at high frequency (every 2 s).

The increased stability of the microheater platform results in a propane sensor with improved response stability. As seen in figure 8, the Pt-BN SiC sensor response is highly stable over a 36 h period of extended continuous operation at 500 °C where the sensor is alternately exposed to clean air and various concentrations of propane. Figure 8 only shows the response to 2% propane for clarity, even though the sensor is exposed to varied concentrations during this test. The response stability is also compared to that of the Pt-BN on a polysilicon microheater and platinum nanoparticle-loaded graphene aerogel (Pt-GA) on a polysilicon microheater. The graphene aerogel has been shown to burn off of the microheater during testing [24], which explains the precipitous drop in response over only a few hours. The Pt-BN on polysilicon fares better but still shows a 15% change in the first 18 h and no visible loss of material, leaving the source of decrease unclear. Given that the Pt-BN SiC sensor uses the same catalytic material but shows no change in response over 36 h, it is likely that the instability in the polysilicon microheater resistance causes an unreliable propane response. For practical use, a stable sensor response would need to be demonstrated over a much longer time period, but even in the first 36 h, the benefit of using silicon carbide as the microheater material is clear. In the same way that the choice of a more thermally stable aerogel material (boron nitride instead of graphene) improved the response stability on the same microheater platform, the choice of a more thermally stable microheater material (silicon carbide instead of polysilicon) demonstrates significant benefit for sensor reliability.

The Pt-BN SiC sensor maintains good propane response when the relative humidity level is increased to 40 and 60% (figure 9(a)). At the highest propane concentrations, the response is a bit higher as the humidity level increases. This may be caused by the lower effective concentration of oxygen at higher humidity levels. As seen in figure 9(b), the sensor response to 5000 ppm propane changes drastically with varied oxygen concentration. The largest response is around 3% oxygen, which is close to the stoichiometric ratio of oxygen to propane for complete combustion (5:1, $C_3H_8 + 5O_2 \rightarrow 3CO_2 + 4H_2O$). The same behavior is reported in catalysis literature on propane oxidation by platinum catalysts [34, 35]. The suggested reason for the decrease in catalytic activity with an oxygen-to-propane ratio above the stoichiometric ratio is the competitive adsorption of oxygen on the platinum surface that limits the access of propane molecules [34]. In the presence of increased relative humidity, the effective oxygen concentration may be lower than the delivered 20%, which would lead to an increase in the sensor response. Functionally, this suggests that for accurate propane detection, the catalytic gas sensor must be paired with an oxygen sensor. However, for a simple alarm for leak detection, an increased propane concentration displaces some of the oxygen, giving a larger sensor response as the leak worsens.

In addition to propane, the Pt-BN SiC sensor also responds to hydrogen gas (figure 9(c)). The sensitivity for hydrogen is larger than for propane even though the combustion energy per mole of gas is lower for hydrogen. This is probably due to the faster reaction kinetics. For some catalytic gas sensing applications, this lack of selectivity may be allowable, as the sensor warns of any potential combustible gas. To improve the selectivity, it is possible to measure the sensor response at various operating temperatures and using analysis such as principal component analysis, determine the contribution of each gas in the mixture to the total response [36–38]. Each gas has a unique response curve with temperature; for example, hydrogen gas has a high response starting at temperatures of 300 °C [26]. The fast thermal response of the microheater can allow for rapid scanning through various operating temperatures. Further improvements in catalyst design may also allow for more selective measurements.

4. Conclusion

Catalytic gas sensors with low power consumption are possible with a miniaturized microheater platform, but stable and reliable performance is critical for practical use. This paper shows that changing from a polysilicon microheater to one fabricated with polycrystalline silicon carbide gives improved performance during high temperature operation. The SiC microheater retains a low power consumption (20 mW for 500 °C) and a high temperature coefficient of resistance, which is important for sensing. It also shows much more stable resistance during continuous heating at 500 °C and during temperature changes from 500 °C up to 650 °C when compared to the polysilicon microheater platform. When a thermally stable catalytic material (in this case, platinum nanoparticle-loaded boron nitride aerogel) is added, the SiC microheater element acts as a catalytic gas sensor element with good sensitivity and response stability for propane detection. Fast response and recovery time (~1 s) is demonstrated, as well as minimal impact when sensing in a humid environment. With no loss in sensitivity during 10% duty cycling, the power consumption can be decreased to 2 mW with data still collected every 2 s. Even within the same microheater design, the choice of heater material can have a large impact on the performance of the catalytic gas sensor. The improved reliability of the SiC-based catalytic gas sensor makes wireless monitoring of combustible gases much more practical and feasible.

Acknowledgments

The authors would like to thank Dr Qin Zhou and Dr Jiyoung Chang for assistance with the design and fabrication process development of the polysilicon microheater, Lunet Luna for assistance with the silicon carbide processing, and Thang Pham for synthesis of the Pt-BN. All the microheater fabrication took place at the Marvell Nanofabrication Laboratory at the University of California, Berkeley. The authors also thank Dr William Mickelson and Dr Marcus Worsley for helpful discussions. This work is supported by the Berkeley Sensor & Actuator Center (BSAC) Industrial Members and the National Science Foundation: Accelerating Innovation Research-Technology Transfer program (IIP 1444950), which provided for design of experiments, microheater fabrication, and sensor performance characterization. AZ acknowledges the Air Force Office of Scientific Research under contract FA9550-14-1-0323, which provided for Pt-BN synthesis route optimization. AH-T and HL acknowledge further support from the NSF Graduate Research Fellowship (DGE 1106400) and the China Scholarship Council, respectively.

References

[1] Bársony I, Ducso C and Furjes P 2009 Thermometric gas sensing *Solid State Gas Sensing* (Boston, MA: Springer) pp 237–60

[2] Gelin P and Primet M 2002 Complete oxidation of methane at low temperature over noble metal based catalysts: a review *Appl. Catal.* B **39** 1–37

[3] Gall M 1991 The Si planar pellistor: a low-power pellistor sensor in Si thin-film technology *Sensors Actuators* B **4** 533–8

[4] Bársony I, Adam M, Furjes P, Lucklum R, Hirschfelder M, Kulinyi S and Ducso C 2009 Efficient catalytic combustion in integrated micropellistors *Meas. Sci. Technol.* **20** 124009

[5] Karpov E E, Karpov E F, Suchkov A, Mironov S, Baranov A, Sleptsov V and Calliari L 2013 Energy efficient planar catalytic sensor for methane measurement *Sensors Actuators* A **184** 176–80

[6] Xu L, Li T, Gao X and Wang Y 2011 Development of a reliable micro-hotplate with low power consumption *IEEE Sens. J.* **11** 913–9

[7] Courbat J, Briand D and de Rooij N F 2008 Reliability improvement of suspended platinum-based micro-heating elements *Sensors Actuators* A **1** 284–91

[8] Briand D, Beaudoin F, Courbat J, de Rooij N F, Desplats R and Perdu P 2005 Failure analysis of micro-heating elements suspended on thin membranes *Microelectron. Reliab.* **45** 1786–9

[9] Ehmann M, Schubert F, Ruther P and Paul O 2002 Thermally activated ageing of polysilicon *IEEE Sens.* **1** 601

[10] Ehmann M, Ruther P, von Arx M, Baltes H and Paul O 2001 Ageing behavior of polysilicon heaters for CMOS microstructures operated at temperatures up to 1200 K *Proc. of the 14th IEEE Int. Conf. on Microelectromechanical Systems (Interlaken, Switzerland, 21–25 January 2001)* pp 147–50

[11] Grudin O, Marinescu R, Landsberger L, Cheeke D and Kahrizi M 1999 Microstructure release and test techniques for high-temperature micro hotplate *Proc. of the 1999 IEEE Canadian Conf. on Electrical and Computer Engineering (Edmonton, Canada, May 9–12 1999)* pp 1610–5

[12] Paul O and Ruther P 2003 Testing the limits of silicon technology based MEMS materials *Proc. of the 2003 Int. Symp. on Micromechatronics and Human Science (19–22 October 2003)* pp 1–9

[13] Maboudian R, Carraro C, Senesky D G and Roper C S 2013 Advances in silicon carbide science and technology at the micro- and nanoscales *J. Vac. Sci. Technol.* A **31** 050805

[14] Chen L and Mehregany M 2009 An examination of material-related performance in SiC heated elements for IR emitter and sensor applications *Mater. Sci. Forum* **600** 863–6

[15] Chung G-S and Jeong J-M 2010 Fabrication of micro heaters on polycrystalline 3C-SiC suspended membranes for gas sensors and their characteristics *Microelectron. Eng.* **87** 2348–52

[16] Solzabacher F, Imawan C, Steffes H, Obermeier E and Moller H 2000 A modular system of SiC-based microhotplates for the application in metal oxide gas sensors *Sensors Actuators* B **64** 95–101

[17] Solzabacher F, Imawan C, Steffes H, Obermeier E and Eickhoff M 2001 A highly stable SiC based microhotplate NO_2 gas sensor *Sensors Actuators* B **78** 216–20

[18] Saxena G and Paily R 2015 Performance improvement of square microhotplate with insulation layer and heater geometry *Microsyst. Technol.* **21** 2331–8

[19] Wiche G, Berns A, Steffes H and Obermeier E 2005 Thermal analysis of silicon carbide based micro hotplates for metal oxide gas sensors *Sensors Actuators* A **123** 12–7

[20] Korlyakov A V and Luchinin V V 1998 Silicon carbide microheater *The 4th Int. High Temperature Electronics Conf. (Albuquerque, NM, June 14–18 1998)* pp 322–3

[21] Chung G-S and Jeong J-M 2010 Fabrication and characteristics of micro heaters based on polycrystalline 3C-SiC for high temperature and voltage *Mater. Sci. Forum* **645** 1085–8

[22] Morana B, Santagata F, Mele L, Mihailovic M, Pandraud G, Creemer J F and Sarro P M 2011 A silicon carbide MEMS microhotplate for nanomaterial characterization in TEM *The 24th Int. Conf. on Microelectromechanical Systems (Cancun, Mexico, January 23–27 2011)* pp 380–3

[23] Noh S, Seo J and Lee E 2009 The fabrication by using surface MEMS of 3C-SiC micro-heaters and RTD sensors and their resultant properties *Trans. Electr. Electron. Mater.* **10** 131–4

[24] Harley-Trochimczyk A, Chang J, Pham T, Dong J, Worsley M A, Zettl A, Mickelson W and Maboudian R 2015 Low power microheater-based combustible gas sensor with graphene aerogel catalyst support *Technical Digest of the 18th Int. Conf. on Solid-State Sensors, Actuators, and Microsystems (Anchorage, AL, June 21–25 2015)* pp 1483–6

[25] Harley-Trochimczyk A, Pham T, Chang J, Chen E, Worsley M A, Zettl A, Mickelson W and Maboudian R 2016 Platinum nanoparticle loading of boron nitride aerogel and its use as a novel material for low-power catalytic gas sensing *Adv. Funct. Mater.* **26** 433–9

[26] Harley-Trochimczyk A, Chang J, Zhou Q, Dong J, Pham T, Worsley M A, Maboudian R, Zettl A and Mickelson W 2015 Catalytic hydrogen sensing using microheated platinum nanoparticle-loaded graphene aerogel *Sensors Actuators* B **206** 399–406

[27] Liu F, Carraro C, Pisano A P and Maboudian R 2010 Growth and characterization of nitrogen-doped polycrystalline 3C-SiC thin films for harsh environment MEMS applications *J. Micromech. Microeng.* **20** 035011

[28] Gao D, Howe R T and Maboudian R 2003 High-selectivity etching of polycrystalline 3C-SiC films using HBr-based transformer coupled plasma *Appl. Phys. Lett.* **82** 1742–44

[29] Zhou Q, Sussman A, Chang J, Dong J, Zettl A and Mickelson W 2015 Fast response integrated MEMS microheaters for ultra low power gas detection *Sensors Actuators* A **223** 67–75

[30] Zhang J, Howe R T and Maboudian R 2006 Electrical characterization of n-type polycrystalline 3C-silicon carbide thin films deposited by 1,3-disilabutane *J. Electrochem. Soc.* **153** G548–51

[31] Bralla J G 2007 *Gas, liquified petroleum (LPG) Handbook of Manufacturing Processes—How Products, Components and Materials are Made* (New York: Industrial Press)

[32] Nolan D P 2011 *Handbook of Fire and Explosion Protection Engineering* 3rd edn (Amsterdam: Elsevier)

[33] Dücso C, Adam M, Furjes P, Hirschfelder M, Kulinyi S and Barsony I 2003 Explosion-proof monitoring of hydrocarbons by mechanically stabilised, integrable calorimetric microsensors *Sensors Actuators* B **95** 189–94

[34] Chiba A, Komoda M, Kosumi T, Nanba T, Azuma N and Ueno A 1999 Difference in catalytic combustion of propane and propene on Pt/Al_2O_3 catalyst *Chem. Lett.* **28** 801–2

[35] Bijjula K and Dimitrios K C 2008 Gaseous reactive flows around catalytically combusting micro-wires *PhD Dissertation* University of Illinois Urbana-Champaign

[36] Engel M, Baumbach M, Kammerer T and Schutze A 2004 Preparation of microstructured pellistors and their application for fast fuel vapor discrimination *The 17th Int. Conf. on Microelectromechanical Systems (Maastricht, Netherlands, January 25–29 2004)* pp 268–71

[37] Huang X, Mend F, Pi Z, Xu W and Liu J 2004 Gas sensing behavior of a single tin dioxide sensor under dynamic temperature modulation *Sensors Actuators* B **99** 444–50

[38] Gramm A and Schutze A 2003 High performance solvent vapor identification with a two sensor array using temperature cycling and pattern classification *Sensors Actuators* B **95** 58–65